JOURNAL OF ENDOUROLOGY
Volume 24, Number 11, November 2010

Pp. 1875–1881
DOI: 10.1089/end.2009.0567

Acoustic Access to the Prostate for Extracorporeal Ultrasound Ablation

Timothy L. Hall, Ph.D.,[1] Christopher R. Hempel, M.D.,[1] Brian J. Sabb, M.D.,[2] and William W. Roberts, M.D.[1]

Abstract

This study aimed to measure acoustic access to the prostate for extracorporeal ultrasound ablation. Both transabdominal and transperineal approaches were considered. The objective was to measure the size and shape of the aperture available for unobstructed targeting of the prostate. CT images of 17 randomly selected men >56 years of age were used to create 3D reconstructions of the lower abdomen and pelvis. Rays were traced from target locations in the prostate toward the perineum and the abdomen. The maximum CT density encountered along each path was recorded; those paths that traversed structures with CT density exceeding a soft tissue threshold were considered to be blocked by bone. Unblocked rays comprised the accessible aperture. The aperture through the perineum was found to be a triangular-shaped region bounded by the lower bones of the pelvis varying significantly in size between subjects. The free aperture through the abdomen was wedge shaped limited by the pubis and also with great subject-to-subject variability. Average unblocked fractions of an f/1 transducer to target base, middle, and apex of the prostate along the urethra from the perineum were 77.0%, 94.4%, and 99.6%, respectively. Averages targeting from the abdomen were 86.1%, 52.3%, and 11.0%. Acoustic access to the prostate for therapy through the perineum was judged to be feasible. Access from the abdomen was judged to be sufficient for the base of the prostate, but likely inadequate for the middle and apex.

Introduction

Histotripsy is a method of ultrasound therapy using brief, intense, focused bursts of ultrasound at a low duty cycle (often below 1%) to cause the formation of microscopic bubbles within tissue—a process known as cavitation. As well as forming microbubbles, the sound field causes them to oscillate violently and collapse releasing large amounts of energy in localized regions. This leads to disruption of cells and tissue structures when applied to solid masses[1,2] and erosion at tissue–fluid interfaces.[3] Provided that the sound field is sufficiently highly focused, intervening tissue will be largely unaffected (as with lithotripsy) yielding a method for targeted noninvasive surgery. Where a sufficient number of histotripsy ultrasound bursts are applied, the targeted tissue is completely fractured, leaving a uniform cavity containing liquefied tissue corresponding to the location of the acoustic focal zone. The margins can be quite sharp—from a few millimeters to <1 millimeter depending on the tissue and properties of the sound field.[1,4] Microbubbles also behave as highly nonlinear absorbers of ultrasound greatly enhancing heating to the point of thermal ablation for continuously applied high-intensity ultrasound.[5,6] Keeping the duty cycle low as is done for histotripsy prevents accumulation of this heat, which would complicate a controlled focal therapy. The lack of heating as a mechanism for tissue destruction is a major distinction between histotripsy and ultrasound thermal ablation, sometimes referred to as high-intensity focused ultrasound (HIFU).

Histotripsy technology is being developed as a noninvasive therapy for benign prostatic hyperplasia (BPH) that will replicate the anatomic result achieved with transurethral resection of prostate. Lake demonstrated feasibility by disrupting prostate tissue with a transabdominal therapy transducer in a canine model.[7] A portion of the glandular prostate and urethra was targeted with histotripsy and fractionated. When flushed, the result was a cavity or enlarged urinary channel within the prostate shown by histology and retrograde urethrography.

An important consideration for translating histotripsy for treatment of BPH in humans is the availability of an acoustic window to access the prostate. Ultrasound is highly attenuated and reflected by bone so that available targets for ultrasound therapy must have clear paths from the skin passing

Departments of [1]Urology and [2]Radiology, University of Michigan, Ann Arbor, Michigan.

through only soft tissues. More specifically, the angle of entry for sound from a focused source to reach a target within the body unobstructed by bone will determine the focal power of the transducer. As histotripsy requires very intense acoustic pulses, it is best to use as highly focused a therapy transducer as possible. This reduces the required surface acoustic power for the transducer, minimizes the overall transducer size, reduces the focal zone for increased precision, and reduces intensity at the skin surface. Experience from lithotripsy suggests that keeping the skin intensity low will improve patient tolerance and reduce the anesthesia requirement.[8,9] For most canines, the prostate is located cranial to the pubis 2 to 3 cm below the skin of the lower abdomen. This makes a transabdominal ultrasound therapy approach relatively straightforward. The human prostate is located deeper within the pelvis, closer to the perineum, suggesting that a transperineal approach could be possible or even preferred.

The aim of this study was to simulate and assess ultrasound access to the human prostate through the perineum and through the abdomen to determine the feasibility of extracorporeal histotripsy prostate ablation.

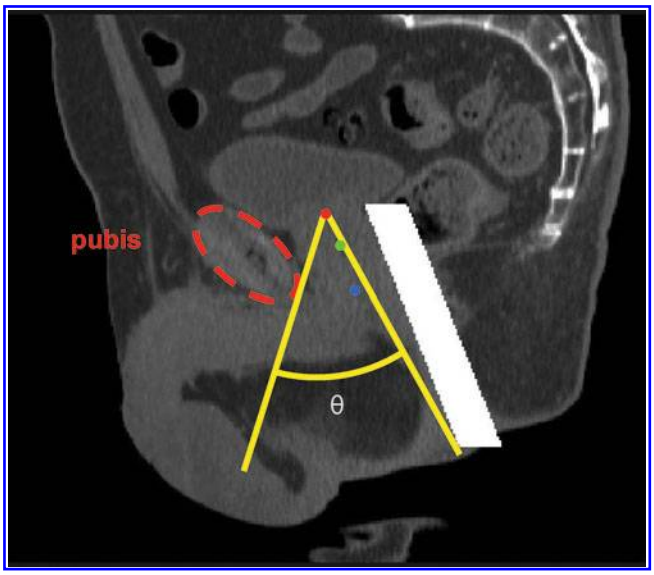

FIG. 1. Sagittal plane image of the pelvic region with target locations marked at the base of prostate (red), midprostate (green), and apex (blue). The white bar simulates a 20-mm-diameter transrectal imaging probe. This centrally located image plane cuts through the pubic symphysis, which only has moderate X-ray density. The angle θ (yellow) represents the clear angle of access to the base of the prostate in this plane bounded by the pubis and rectum.

Materials and Methods

After receiving IRB approval, digital imaging and communications in medicine (DICOM) image data were collected from 23 randomly selected patients undergoing arterial contrast-enhanced CTs. These data were de-identified keeping only the subject age and assigning an arbitrary reference number. Subjects <56 years of age and scans of poor quality were excluded, leaving 17 data sets (mean age 66.4) for transperineal ultrasound access measurement. Two additional subjects were excluded from this set for transabdominal ultrasound access measurement because of high levels of CT contrast within the bladder, leaving a set of 15 (mean age 67.5). For each subject, 40 to 50 image planes (1.25 mm spacing and 0.8 mm in-plane resolution) spanning the lower abdomen and pelvis were imported into MATLAB (The Mathworks, Natick, MA) and resampled to an isotropic 1 mm resolution. Prostate dimensions were measured (height, width, and length) on the reconstruction and used to calculate volume using an ellipsoid approximation. The range and mean volumes were 25.2 to 68.4 cm^3 and 41.3 cm^3, respectively. Target locations at the base, midprostate, and apex of the prostate of each subject were marked by one of the authors independent of subsequent data analysis. Additionally, a 20-mm-diameter cylindrical mask simulating a transrectal imaging probe (GE model ERB) was placed appropriately in the reconstruction as this could presumably block ultrasound therapy propagation along certain paths. An example is shown in Figure 1.

From each subject and target location, 1001 evenly spaced rays spanning a 120° solid angle were traced toward the perineum. The maximum CT density encountered along each path (ray) was recorded with those exceeding a soft tissue threshold assumed to be blocked by bone. The threshold used was approximately midway between typical CT density observed for bone and that for skeletal muscle with the intention of generating a close approximation of the bony pelvis. The remaining unblocked rays comprised the total available transducer aperture. The process was repeated for rays targeted toward the abdomen. Transabdominal rays exceeding 30° (instead of 60°) from normal toward the upper body were excluded as these would likely begin to impinge on the bowel and would require excessive compression on the abdomen from a therapy transducer. In both cases, ray positioning was based on a geodesic dome arrangement, which produced a uniform sampling of theoretical curved transducer apertures. For example, a transducer with a focal distance of 100 mm using this ray density produces a pseudohexagonal sampling with a mean spacing of 5.5 mm. A rendering of the skeleton of one subject and the ray tracing process is shown in Figure 2. A similar ray tracing algorithm for defining effective elements of a transducer array in the planning of ultrasound thermal ablation was described by McGough.[10]

The 120° aperture is much greater than typically required for an ultrasound therapy transducer (equivalent to f-number = 0.6, i.e., the ratio between the focal length and diameter) and was taken to represent the collection of all reasonable transducer placement locations for a smaller transducer pointed directly at the target. To simulate a more realistic size transducer, for each target location and subject, a circular region spanning a 60° solid angle (f-number = 1) was placed within the overall aperture such that the number of unblocked rays was maximized achieving an optimal placement. The fraction of this smaller region unblocked was then used to represent the fraction of the surface of an appropriately placed realistic therapy transducer that would be unblocked in reaching the target. For each of the target locations, the apertures from the subjects were aligned and averaged to create a statistical aperture where each point represented the probability that it was blocked to sound propagation.

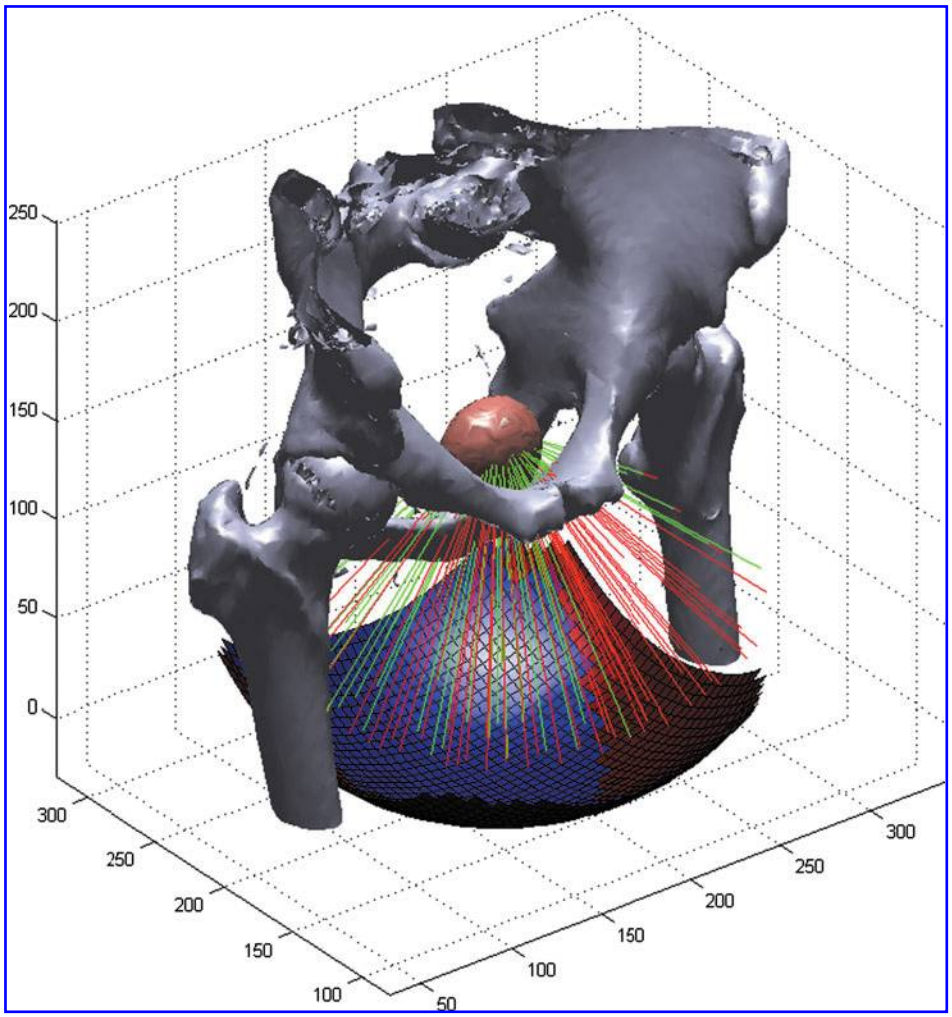

FIG. 2. A sketch of the ray tracing process used to determine free-path access to the prostate. Bones are rendered from high X-ray density locations in a CT dataset. Rays emanate from a target location within the prostate (pink). Those striking bone are considered to be blocked (red lines), whereas those passing through only soft tissue are part of the accessible path (green lines). Blue and red squares below represent the clear and blocked regions of a hypothetical curved transducer surface. For clarity, only a fraction of the 1001 simulated rays are shown.

Results

The overall free aperture through the perineum was a triangular region bounded by bones of the pelvis (pubis and ischial tuberosities) and the location of the transrectal probe and varied significantly in size between subjects (Fig. 3). The free aperture through the abdomen was wedge shaped limited by the pubis and also with great subject-to-subject variability. Average unblocked fractions of the f-number = 1 transducer to target base, midprostate, and apex along the urethra through the perineum were 77.0%, 94.4%, and 99.6%, respectively. Averages targeting through the abdomen were 86.1%, 52.3%, and 11.0%. These data along with ranges and standard deviations are shown in Table 1. Results for midprostate and base of prostate along the urethra are shown for each subject in Figure 4 with scatter plots against prostate volume. For these locations, access appears to be independent of prostate volume.

Additional focal locations away from the urethra were tested with mean available aperture across subjects shown in Figures 5 and 6 for transperineal and transabdominal targeting, respectively. When targeting transperineal, a small reduction in aperture is seen for locations lateral to the urethra, whereas a more significant drop is seen for locations closer to the pubis. For a transabdominal approach, target locations off the urethra result in similar apertures to those on the urethra.

For the 15 subjects where access to the prostate from the abdomen and perineum could be directly compared, 4 had greater access from the perineum to the base of the prostate. All 15 had greater access to the midprostate or apex from the perineum. In general, target locations in the midprostate and apex of the prostate for most subjects were found to have good accessibility from the perineum and limited accessibility from the abdomen. The prostate base was found to be highly accessible from the abdomen and moderately accessible from the perineum. Overall, acoustic access to the full prostate for therapy was judged to be sufficient through the perineum but not the abdomen.

Discussion

The data for this study came from supine cross-sectional images of patients. It is possible that subjects could be positioned in lithotomy for transperineal therapy or supine flexed for transabdominal therapy to make the anatomy more favorable. Filling the bladder via a urinary catheter may also be helpful by displacing the prostate toward the perineum or

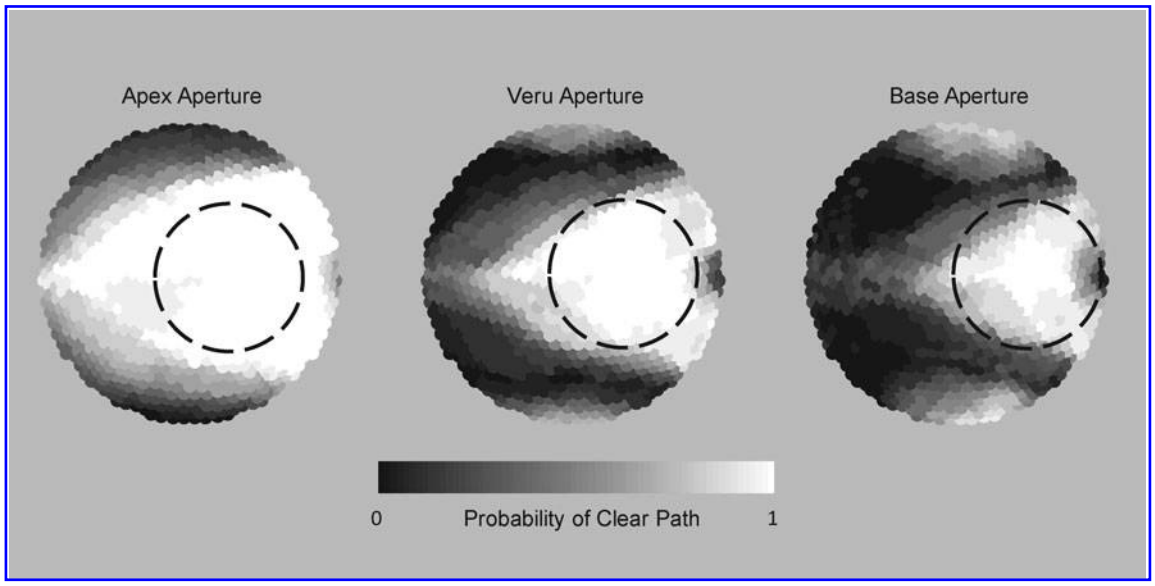

FIG. 3. Statistical combination of free apertures from the perineum for 17 patients targeting various locations in the prostate showing the probability of unblocked access from different angles. The free area is a triangular region bounded by the pelvis (top and bottom edges) and the transrectal imaging probe (right edge). The circular dashed line represents a typical size therapy transducer of f-number = 1 in an optimal placement.

displacing the bowel away from the transabdominal acoustic path. Direct physical manipulation of the prostate with a device in the rectum or urinary catheter in the bladder may also be possible to help bring the prostate closer to the aperture of choice. Thus, this study may be considered to represent a worst-case scenario for acoustic access to the prostate given no attempt to improve positioning.

The status of the subjects in this study with respect to BPH or lower urinary tract symptoms was not available. The range of prostate volumes in this study (25–68 cm^3) is reasonable for many patients with BPH and lower urinary tract symptoms. For prostates with very large median lobes extending into the bladder, the base may be significantly more difficult to access from the perineum. An alternative may be to use a multiple aperture approach for treatment targeting the mid prostate region from the perineum and the base from the abdomen.

The methods used in this study could be repeated for the entire volume of the prostate if desired. However, for this study, this was limited to several representative target locations that were tested on a number of patients. Target points were selected at the midprostate along the urethral axis and at 1 and 2 cm from the urethral axis horizontal, vertically, and at 45°. Similarly, at the base, target points were selected on the urethral central axes and at 1 cm distances vertically, horizontally, and at 45°. These target points were chosen to generally fall within or approximate the margin of planned resection volume for BPH therapy. Points more central than these marginal points are expected to have a greater fraction of aperture available as they are more centrally located with respect to the ring of the bony pelvis. Therefore, if the available aperture is sufficient for therapy at the marginal points, it should also be sufficient at points between this margin and the center point on the urethra.

The methods presented here could be applied to analyze acoustic access for other targets in the body. Additional modeling including absorption is often desirable for thermal ablation methods such as HIFU where heat deposition to bony structures could be a concern.[11]

To design a transducer for ultrasound therapy, the skin surface-to-target distance must be known. Along with the aperture size in terms of angle, these numbers determine the minimum size of a transducer that can be used. Larger transducers are also possible using a longer standoff path between the transducer and the skin surface (usually a fluid-filled container). However, as therapy transducers become significantly more expensive with increasing size, economic

Table 1. Results and Statistics for Acoustic Access to the Prostate Through Transperineal and Transabdominal Windows

Target	*Average free aperture (%)*	*Standard deviation (%)*	*Range (%)*
Transperineal			
Base	77.0	12.2	50.8–96.6
Mid	94.4	4.8	83.7–100
Apex	99.6	0.9	96.2–100
Transabdominal			
Base	86.1	12.6	61.2–100
Mid	52.3	14.6	23.6–76.0
Apex	11.0	10.1	0–30.0

Percentages represent the fraction of a typical therapy transducer surface that would be unblocked by acoustically opaque tissues in reaching that target. The perineal window is sufficient to target the entire prostate for most subjects, whereas the abdominal window is only sufficient for targeting the base.

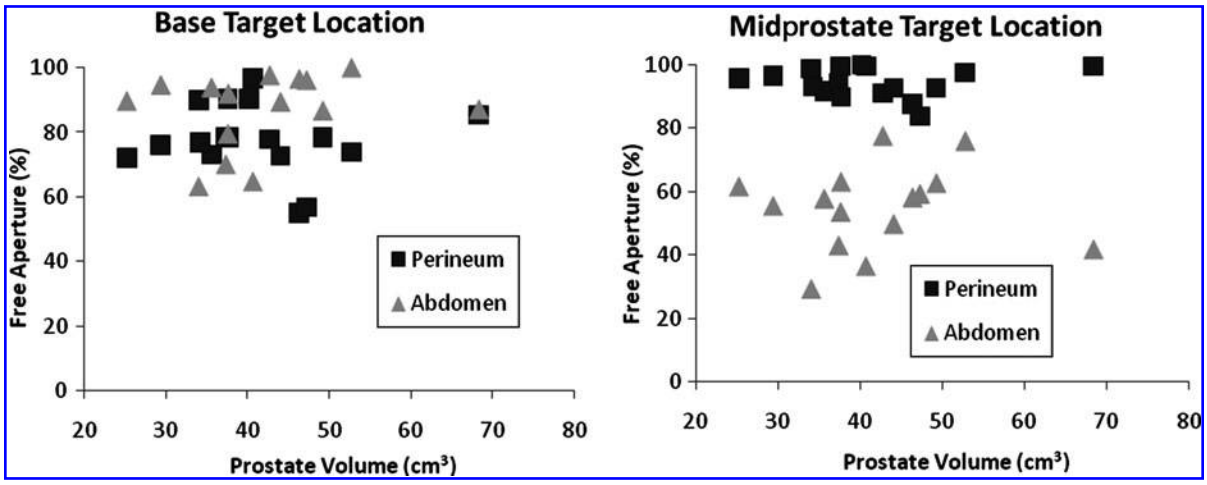

FIG. 4. Scatter plots of free apertures for all subjects plotted against prostate volume for urethral target locations. Subject-to-subject variability appears to outweigh any correlation with prostate volume for these target locations. The base target location favors the transabdominal approach slightly for many subjects; however, the midprostate location greatly favors transperineal for all subjects.

constraints would likely limit the size to the minimum necessary for efficacy. Taking the transperineal path as the most favorable from this study, the perineum-to-prostate base distance needs to be known. The authors were not confident that these data could be determined from the supine cross-sectional images. The perineal skin surface could not always be discerned precisely and the skin and subcutaneous tissues are expected to shift with repositioning to lithotomy position. A study by Häcker et al,[12] where transperineal ultrasound thermal ablation of the prostate (HIFU) was attempted, used a transducer with a 100-mm working distance (front surface to focal point). Prostate lesions were made in eight subjects at depths ranging from 53 to 80 mm. It was not specified where within the prostates these target locations were placed.

In a preliminary unpublished study of three cadavers positioned in lithotomy, skin-to-prostate distance was measured using spinal needles inserted through the perineum under

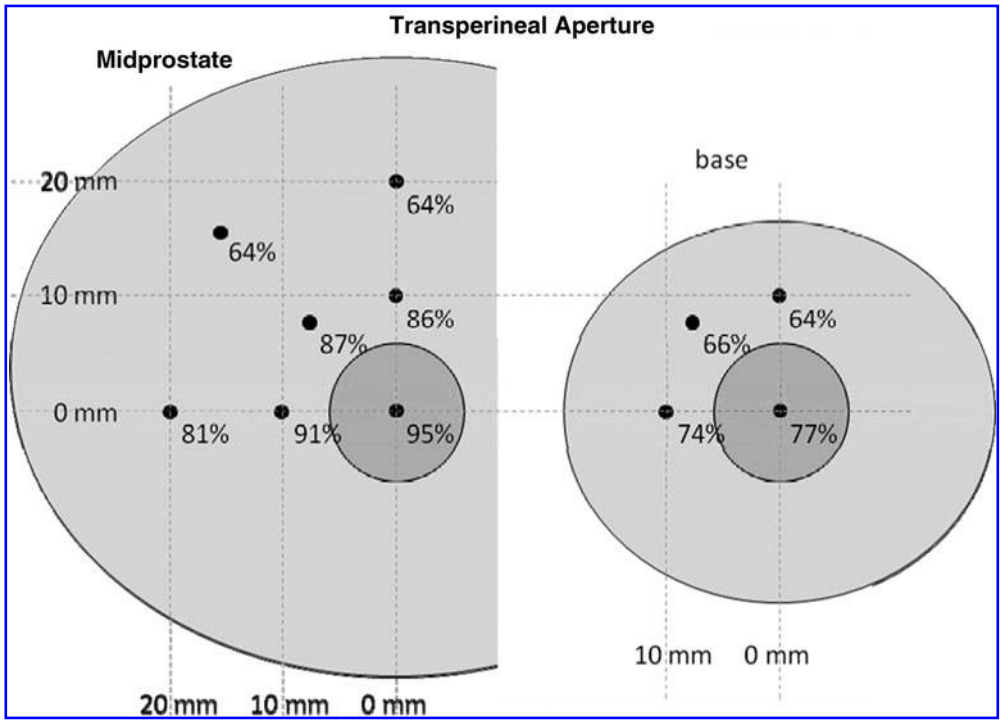

FIG. 5. Mean free apertures for transperineal target locations along the urethra (small circle) and 1 to 2 cm away in the midprostate and base. Locations closer to the pubis are significantly reduced.

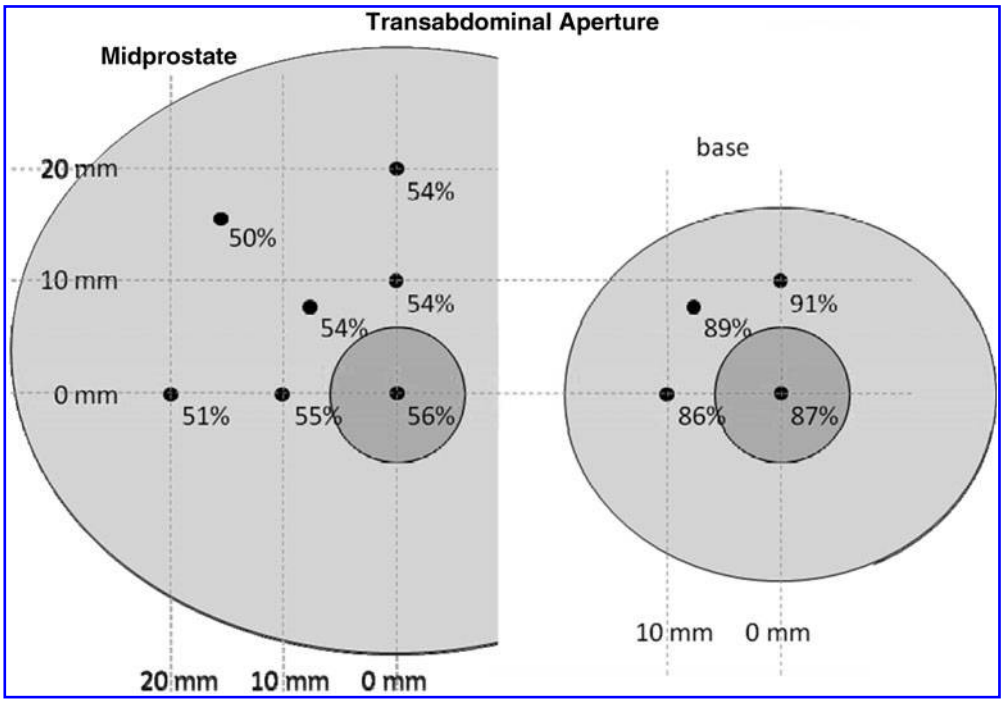

FIG. 6. Mean free apertures for transabdominal target locations along the urethra (small circle) and 1 to 2 cm away in the midprostate and base. Minimal differences are observed for various locations in each plane.

transrectal ultrasound guidance. Skin to apex of prostate distances were found to be 50, 72, and 40 mm. Skin to base of prostate distances were 85, 95, and 83 mm. These seem to be in agreement with the Häcker study suggesting that a transducer working distance of ~100 mm would be sufficient for many subjects.

The specific acoustic parameters (ultrasound frequency, burst length, and repetition rate) and properties of the target tissue have an effect on the pressure threshold to initiate histotripsy. Likewise, the amount of therapy transducer obstruction that can be tolerated will vary. For a relatively small transducer with a 100-mm-diameter aperture and 100 mm working distance, the permissible obstruction is likely 25% or less.

A significant acoustic window exists through the perineum to access the prostate with extracorporeal ultrasound therapy. The apex of the prostate is easily accessed without obstruction. The base of the prostate is partially blocked by bones of the pelvis, but a large fraction of a typical therapy transducer aperture is still available for many subjects, suggesting that this approach is feasible. Transabdominally, the base of the prostate is accessible for most subjects; however, the midprostate and apex of the prostate have limited accessibility.

Acknowledgments

This work was supported in part by grants from the NIH (K08DK081656), The American Urological Association Foundation, Astellas Pharma US, Inc., and the Wallace H. Coulter Foundation. The authors would like to thank Dr. Nicholas Styn for cadaver measurements.

Disclosure Statement

Timothy Hall and William Roberts are inventors of intellectual property licensed to Histosonics, Inc., hold stock in Histosonics, Inc., and consult for Histosonics, Inc. Christopher R. Hempel and Brian J. Sabb have no competing financial interests.

References

1. Roberts WW, Hall TL, Ives K, et al. Pulsed cavitational ultrasound: A noninvasive technology for controlled tissue ablation (histotripsy) in the rabbit kidney. J Urol 2006;175: 734–738.
2. Kieran K, Hall TL, Parsons JE, et al. Refining histotripsy: Defining the parameter space for the creation of nonthermal lesions with high intensity, pulsed focused ultrasound of the *in vitro* kidney. J Urol 2007;178:672–676.
3. Xu Z, Ludomirsky A, Eun LY, et al. Controlled ultrasound tissue erosion. IEEE Trans Ultrason Ferroelectr Freq Control 2004;51:726–736.
4. Hall TL, Kieran K, Ives K, et al. Histotripsy of rabbit renal tissue *in vivo*: Temporal histologic trends. J Endourol 2007; 21:1159–1166.
5. Umemura S, Kawabata K, Sasaki K. *In vivo* acceleration of ultrasonic tissue heating by microbubble agent. IEEE Trans Ultrason Ferroelectr Freq Control 2005;52:1690–1698.
6. Yang X, Roy RA, Holt RG. Bubble dynamics and size distributions during focused ultrasound insonation. J Acoust Soc Am 2004;116:3423–3431.
7. Lake AM, Hall TL, Kieran K, et al. Histotripsy: Minimally invasive technology for prostatic tissue ablation in an *in vivo* canine model. Urology 2008;72:682–686.

8. Coleman AJ, Saunders JE. A survey of the acoustic output of commercial extracorporeal shock wave lithotripters. Ultrasound Med Biol 1989;15:213–227.
9. Schneider HT, Hummel T, Janowitz P, et al. Pain in extracorporeal shock-wave lithotripsy: A comparison of different lithotripters in volunteers. Gastroenterology 1992;102:640–646.
10. McGough RJ, Kessler ML, Ebbini ES, Cain CA. Treatment planning for hyperthermia with ultrasound phased arrays. IEEE Trans Ultrason Ferroelectr Freq Control 1996;43:1074–1084.
11. Nell DM, Myers MRJ. Thermal effects generated by high-intensity focused ultrasound beams at normal incidence to a bone surface. Acoust Soc Am 2010;127:549–559.
12. Häcker A, Köhrmann KU, Back W, et al. Extracorporeal application of high-intensity focused ultrasound for prostatic tissue ablation. BJU Int 2005;96:71–76.

Address correspondence to:
Timothy L. Hall, Ph.D.
Department of Urology
University of Michigan
2200 Bonisteel Blvd.
Ann Arbor, MI 48109

E-mail: hallt@umich.edu

Abbreviations Used

BPH = benign prostatic hyperplasia
CT = computed tomography
DICOM = digital imaging and communications in medicine
HIFU = high-intensity focused ultrasound
IRB = institutional review board

This article has been cited by:

1. Christopher R. Hempel, Timothy L. Hall, Charles A. Cain, J. Brian Fowlkes, Zhen Xu, William W. Roberts. 2011. Histotripsy Fractionation of Prostate Tissue: Local Effects and Systemic Response in a Canine Model. *The Journal of Urology* **185**:4, 1484-1489. [CrossRef]